Convolutional Neural Networks for Detection of Point Source Methane Plumes in Airborne Imaging Spectrometer Data

Kelly O'Neill[1]; Patrick Sullivan[1]; Andrew Thorpe[2]; Riley Duren[3,4]; Philip E. Dennison[1]

[1] University of Utah; [2] NASA Jet Propulsion Laboratory, California Institute of Technology; [3] Carbon Mapper; [4] University of Arizona

Background

Methane

- Atmospheric methane (CH_4) is a potent greenhouse gas responsible for 20% of anthropogenic radiative forcing since 1750 [1]
- Anthropogenic sources constitute 50-65% of CH_4 emissions and in many cases are under estimated in bottom-up emission budgets [2]
- 20-50% of regional budgets may be produced by point-source super-emitters [3]

Detection & Quantification

- CH_4 point-source detection is carried out through the use of matched filter (MF) analysis of airborne hyperspectral imagery [4]
- Integrated methane enhancements (IMEs) of plumes, calculated from MF retrievals and measured in kilograms, are used to derive flux rates [5]
- The identification and masking of plumes from MF outputs is necessary as confuser materials such as roads, roofs, and paints appear as false positives [6]
- Delineation is typically conducted through manual inspection and simple statistical analyses [5-6]

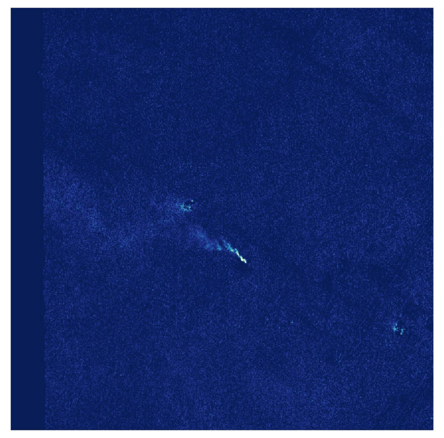

Plume Detection

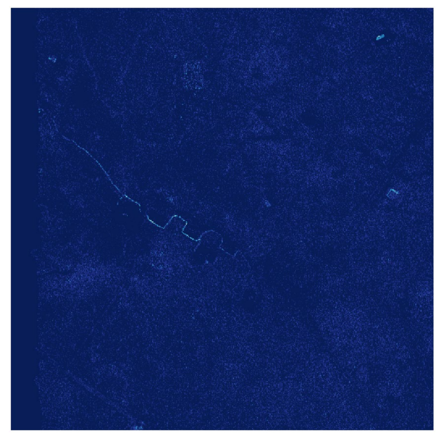

Confusers

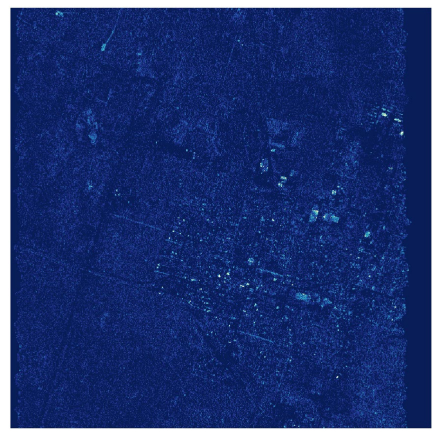

Confusers

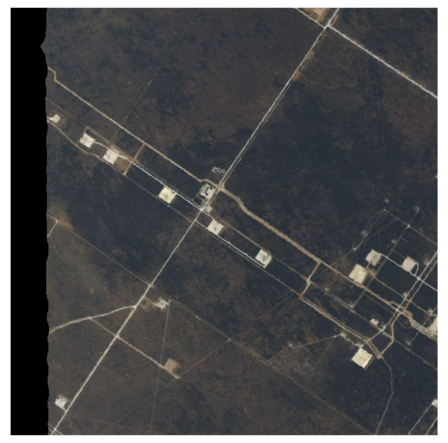

True Color Scene

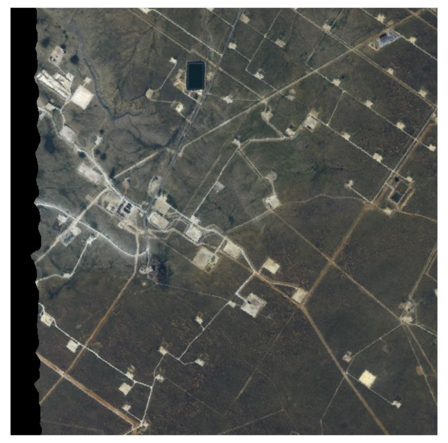

True Color Scene

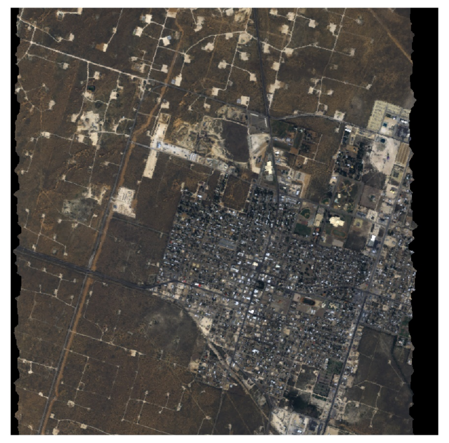

True Color Scene

Convolutional Neural Networks

- Convolutional Neural Networks (CNNs) are a growing interest in remote sensing image classification [7]
- Utilizing moving window sampling CNN models recognize local patterns that are translation invariant and scalable [8]
- Recent fully convolutional neural network (FCNN) architectures allow for the semantic classification of images on a pixel-by-pixel level [9]
- FCNNs have the potential to automate CH_4 plume delineation

Objectives

- Create an FCNN architecture capable of processing spectral bands alongside matched filter inputs
- Train the FCNN for the detection and delineation of methane plumes
- Review feasibility of FCNNs for accurate methane plume delineation

Data

- AVIRIS-NG data were collected during a 2019 flight campaign over the Permian Basin
  - The basin accounts for 38% of US oil and 17% of US natural gas production [10]
  - 380 – 2510nm wavelength range
  - 600 cross track elements
  - 5.6 – 6.0nm sampling range
- Flown for 22 days between September 22nd and October 25th [11]
- Produced 335 flight lines, 274 of which contained CH_4 enhancements [11]

Methods

- FCNN architecture based on U-Net, allowing for pixel-wise semantic segmentation [9]
  - Encoder path increases feature layers while down-sampling image resolution
  - Decoder path uses skip connections to up-sample feature layers to full resolution
- Encoder learns to discriminate plumes from confusers while the decoder learns to reassemble feature layers into semantically classified outputs

- 131 flight lines were reviewed, with plumes manually labeled

Real-Color RGB Scene

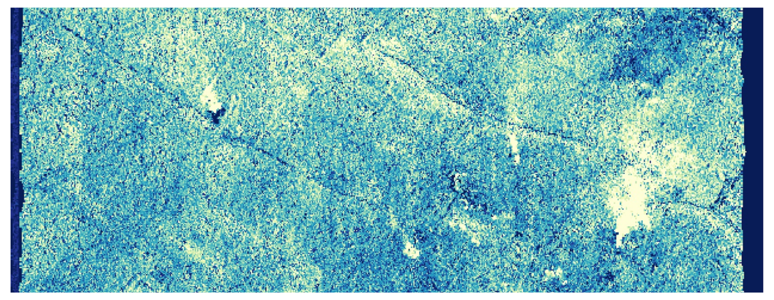

Multi-Modal Matched Filter

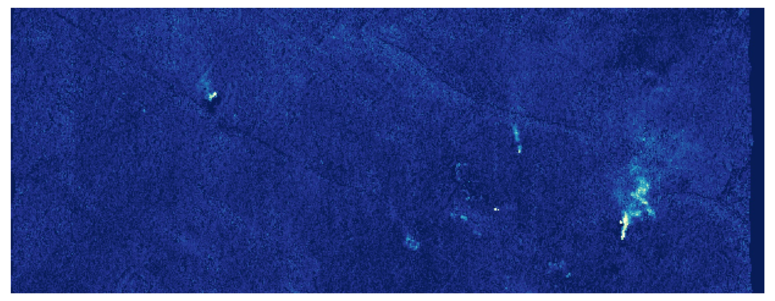

85th – 99.999th Percentile

Labeled Plumes

- Stratified splits of 84 training, 21 testing, and 26 validation scenes were utilized
- Scenes were cropped to 480x480 pixel image tiles containing two bands
  - Single panchromatic band
  - Multi-modal matched filter provided by NASA Jet Propulsion Lab (JPL)
- Tiles from underrepresented scenes were augmented with 50% overlap, horizontal flip, vertical flip, random rotation, and transpose axis to increase training data
- Tiles from well represented scenes were augmented with only 50% overlap and one random rotation
- Model was trained for 47 hours using early stopping, converging at 19 epochs

Results

ang20191017t163235-A

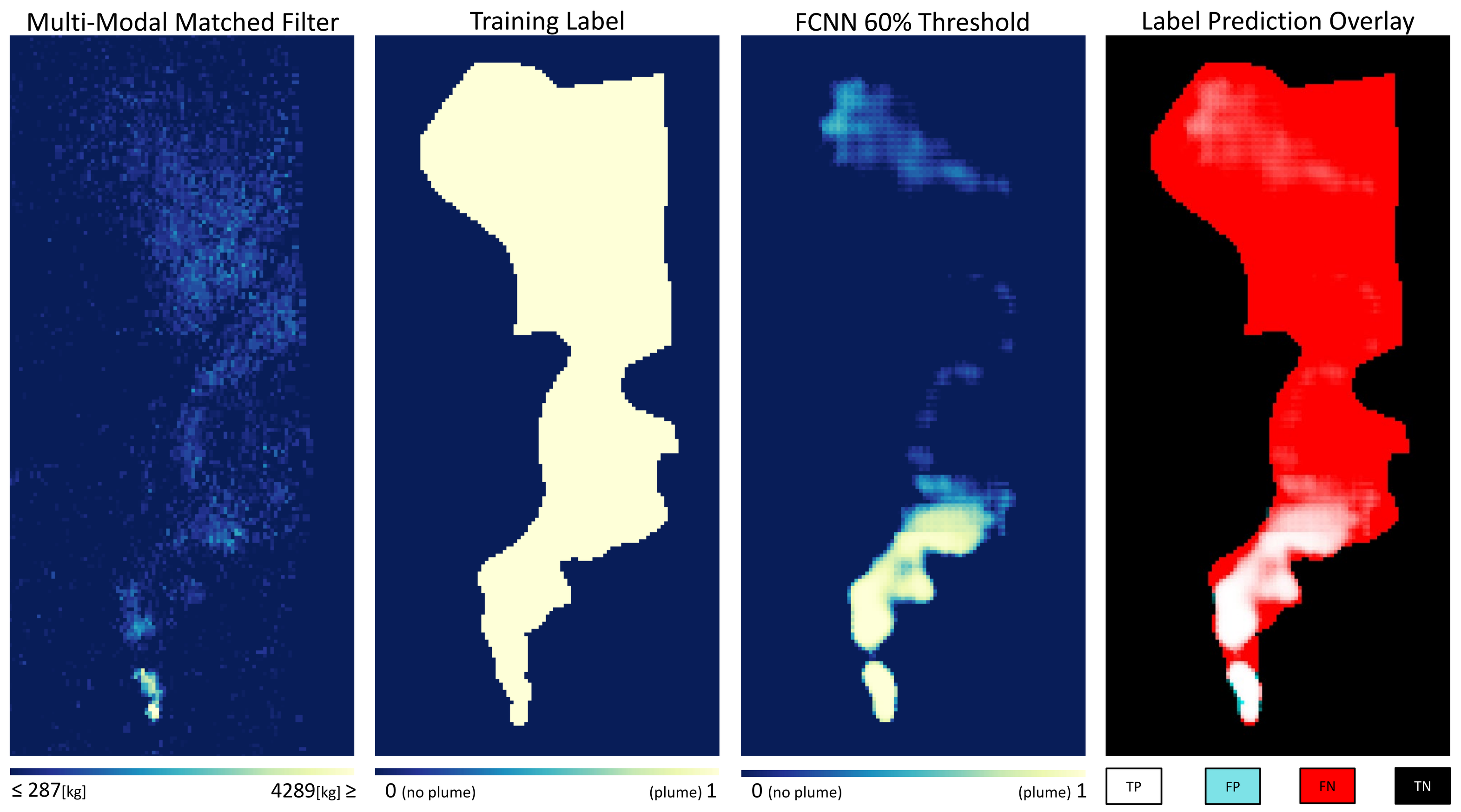

ang20191022t175031-A

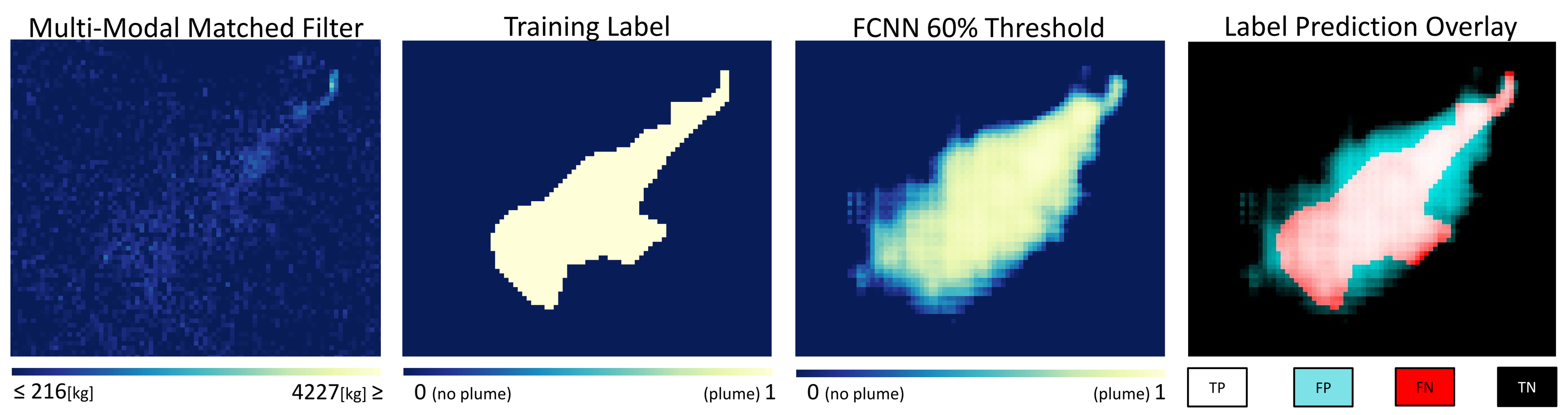

Results cont.

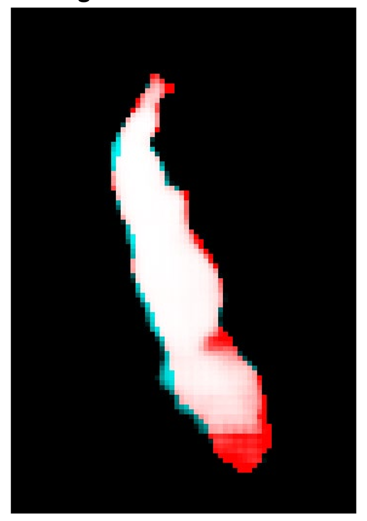

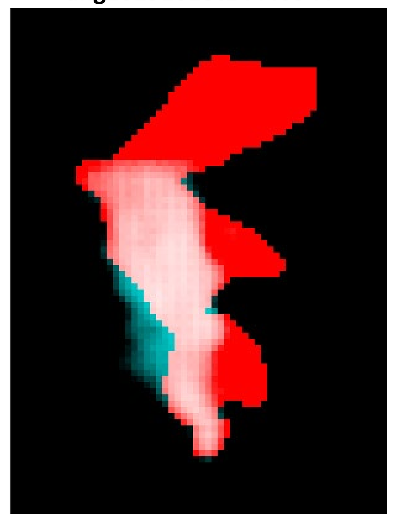

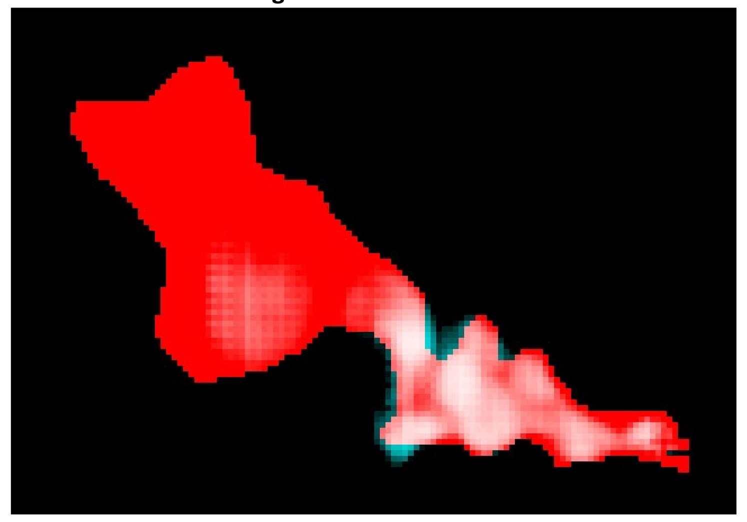

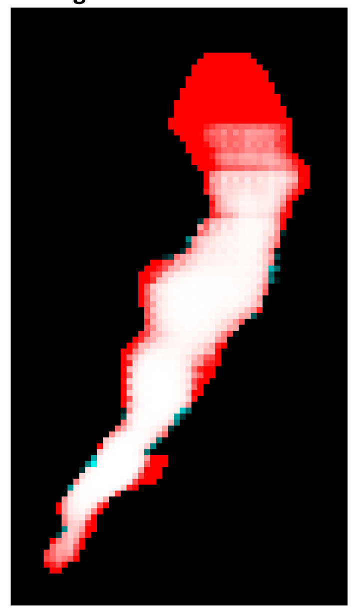

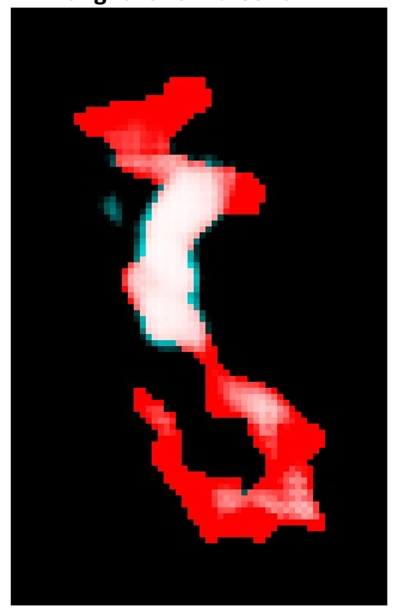

Confusion Matrix: All Validation Scenes

(60% FCNN Threshold)

		Predicted	
		Positive	Negative
Actual	Positive	1,491,393	2,918,146
	Negative	529,861	1,736,886,656

Binary Accuracy: 0.9980 Precision: 0.7379 AUC: 0.9240
Loss: 0.0076 Recall: 0.3382

Example Individual Plume IMEs

Label IME calculated from Training Labels; FCNN IME used a 60% threshold. JPL IME calculated with concentric circles at a 20m fetch. All calculations adopt a 1000ppm-m pixel enhancement cut off for IME inclusion, based on standard JPL IME method. Bolded plumes are shown in figures.

Plume Identifier	Label IME [kg]	FCNN IME [kg]	JPL IME [kg]
ang20191017t163235-A	40.79	20.42	7.04
ang20191018t144405-A	24.33	19.91	35.38
ang20191016t153826-A	20.30	16.60	15.80
ang20191017t174946-A	11.85	11.77	10.97
ang20191019t153454-A	7.39	7.49	7.33
ang20191021t183204-A	7.36	4.97	7.72
ang20191017t152518-A	5.65	4.52	3.83
ang20191017t152518-B	5.62	4.95	5.54
ang20191016t165454-A	4.08	3.96	3.70
ang20191022t175031-A	2.04	2.03	1.06
ang20191017t163235-B	1.08	0.91	1.05
ang20191021t183204-B	0.80	0.61	0.63

Plume Identifier	Label IME [kg]	FCNN IME [kg]	JPL IME [kg]
ang20191016t165454-B	55.70	54.77	--
ang20191017t163235-C	2.88	2.88	--
ang20191017t174946-B	--	22.10	21.07
ang20191017t152518-C	--	3.89	4.19
ang20191016t152245-A	2.96	--	1.25
ang20191016t152245-B	1.43	--	1.05
ang20191022t175031-B	1.29	--	--
ang20191022t172245-C	0.19	--	--
ang20191016t153826-C	--	17.68	--
ang20191022t172245-A	--	0.84	--
ang20191016t165454-C	--	--	0.47
ang20191022t175031-B	--	--	0.85

Conclusions

- FCNNs can be trained for the delineation of plumes from matched filter outputs
- Plume morphology allows for the exclusion of typical human-built confusers
- IME values are comparable to previous manually derived values provided by JPL
- FCNN predictions are computationally and time efficient once a model is trained, taking roughly one minute per scene

Future Work

- Determine optimal IME and FCNN thresholds for pixel identification and masking
- Label and train on scenes with heterogenous landscapes to increase robustness
- Automate the IME calculation of individual plumes from predicted scenes

References

1. M. Saunois, P. Bousquet, B. Poulter, et all, "The global methane budget 2000 - 2012," Earth System Science Data, vol. 8, no. 2, pp. 697–751, 2016. [Online]. Available: https://www.earth-syst-sci-data.net/8/697/2016/
2. Varon, D. J., McKeever, J., Jervis, D., Maasakkers, J. D., Pandey, S., Houweling, S., et al. (2019). Satellite discovery of anomalously large methane point sources from oil/gas production. Geophysical Research Letters, 46 (22), 13507–13516. https://doi.org/10.1029/2019gl083798
3. Duren, R. M., Thorpe, A. K., Foster, K. T., Rafiq, T., Hopkins, F. M., Yadav, V., et al. (2019). California's methane super-emitters. Nature, 575 (7781), 180–184. https://doi.org/10.1038/s41586-019-1720-3
4. Frankenberg, C., Thorpe, A. K., Thompson, D. R., Hulley, G., Kort, E. A., Vance, N., et al. (2016). Airborne methane remote measurements reveal heavy-tail flux distribution in four corners region. Proceedings of the National Academy of Sciences, 113 (35), 9734–9739. https://doi.org/10.1073/pnas.1605617113
5. Varon, D. J., Jacob, D. J., McKeever, J., Jervis, D., Durak, B. O. A., Xia, Y., & Huang, Y. (2018). Quantifying methane point sources from fine-scale satellite observations of atmospheric methane plumes. Atmospheric Measurement Techniques, 11 (10), 5673–5686. https://doi.org/10.5194/amt-11-5673-2018
6. Ayasse, A. K., Dennison, P. E., Foote, M., Thorpe, A. K., Joshi, S., Green, R. O., et al. (2019). Methane mapping with future satellite imaging spectrometers. Remote Sensing, 11 (24), 3054. https://doi.org/10.3390/rs11243054
7. Ma, L., Liu, Y., Zhang, X., Ye, Y., Yin, G., & Johnson, B. A. (2019). Deep learning in remote sensing applications: A meta-analysis and review. ISPRS Journal of Photogrammetry and Remote Sensing, 152, 166–177. https://doi.org/10.1016/j.isprsjprs.2019.04.015
8. Kattenborn, T., Leitloff, J., Schiefer, F., & Hinz, S. (2021). Review on convolutional neural networks (CNN) in vegetation remote sensing. ISPRS Journal of Photogrammetry and Remote Sensing, 173, 24–49. https://doi.org/10.1016/j.isprsjprs.2020.12.010
9. Ronneberger, O., Fischer, P., & Brox, T. (2015). U-net: Convolutional networks for biomedical image segmentation. In Lecture notes in computer science (pp. 234–241). Springer International Publishing. https://doi.org/10.1007/978-3-319-24574-4_28
10. EIA, U. (2018). Drilling productivity report. Production by Region, Accessed December, 13.
11. Cusworth, D. H., Duren, R. M., Thorpe, A. K., Olson-Duvall, W., Heckler, J., Chapman, J. W., et al. (2021). Intermittency of large methane emitters in the permian basin. Environmental Science & Technology Letters, 8 (7), 567–573. https://doi.org/10.1021/acs.estlett.1c00173
12. JPL, U. (2021a). Specifications. AVIRIS Next Generation, Accessed July. Retrieved from avirisng.jpl.nasa.gov/specifications.html

Acknowledgements

- Funding for this research was provided by NASA Carbon Monitoring System Grant 80NSSC20K0244
- We appreciate assistance provided by the NASA JPL AVIRIS-NG team